

ANEXOS E APÊNDICES

APÊNDICES

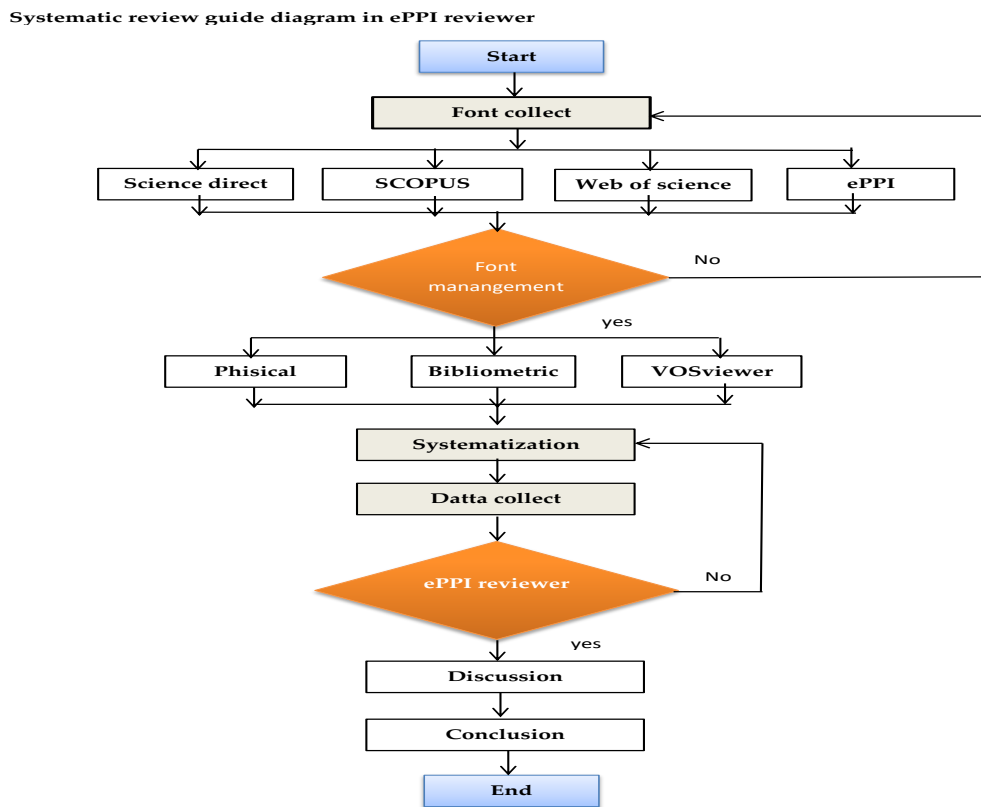


Figura A1: Desenho exploratório de recolha de dados.

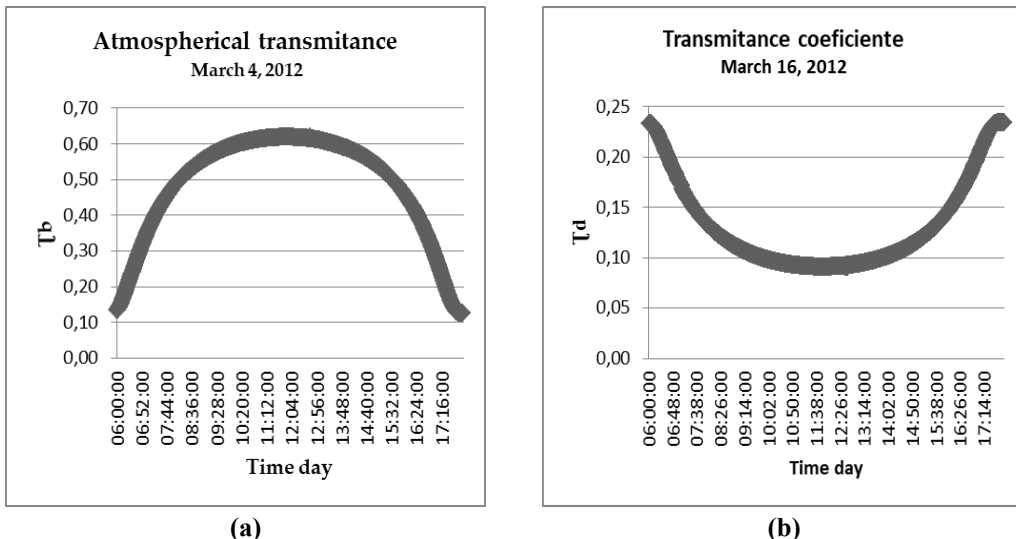


Figura A2: Comportamento da: (a) Transmitância atmosférica e (b) Coeficiente de transmitância.

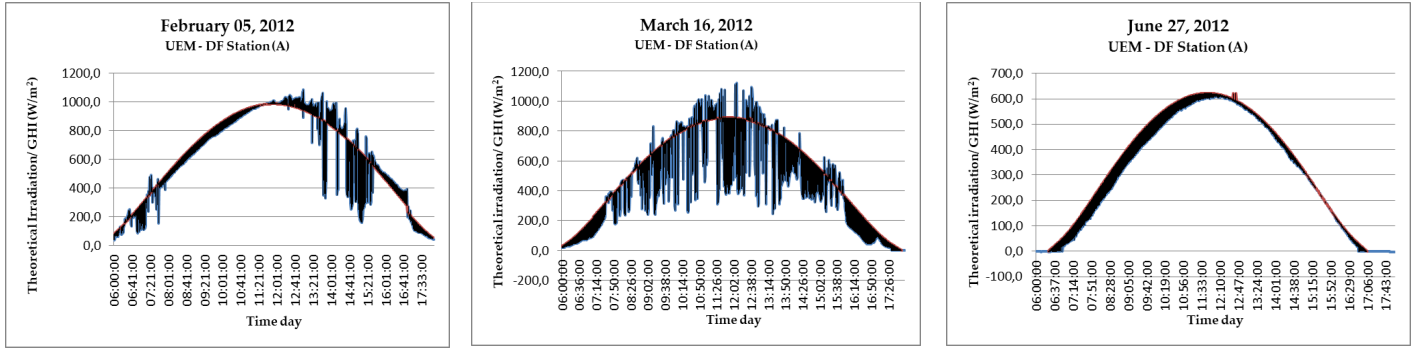


Figura A3: Irradiação teórica em céu limpo: **(a)** $\Delta t=1$ minuto no dia 5 de fevereiro de 2012 e **(b)** $\Delta t=10$ minutos no dia 14 de novembro de 2012 e **(c)** $\Delta t=10$ minutos no dia 30 de junho de 2012 .

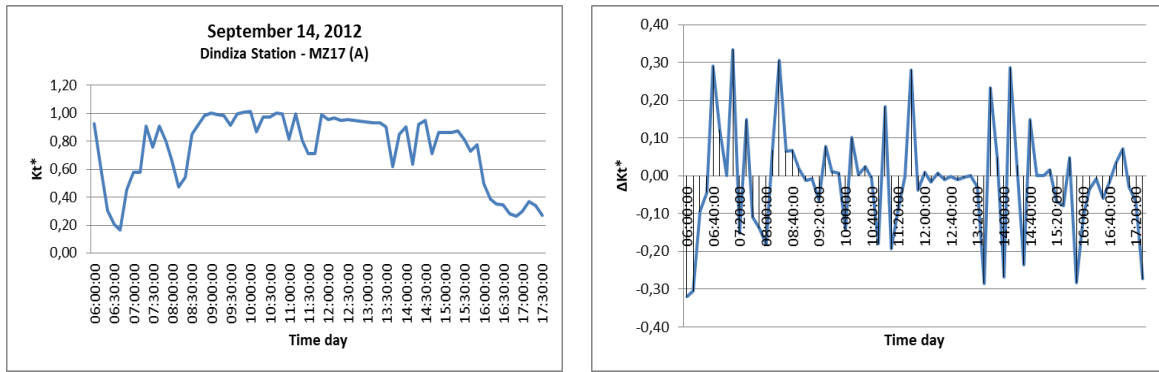
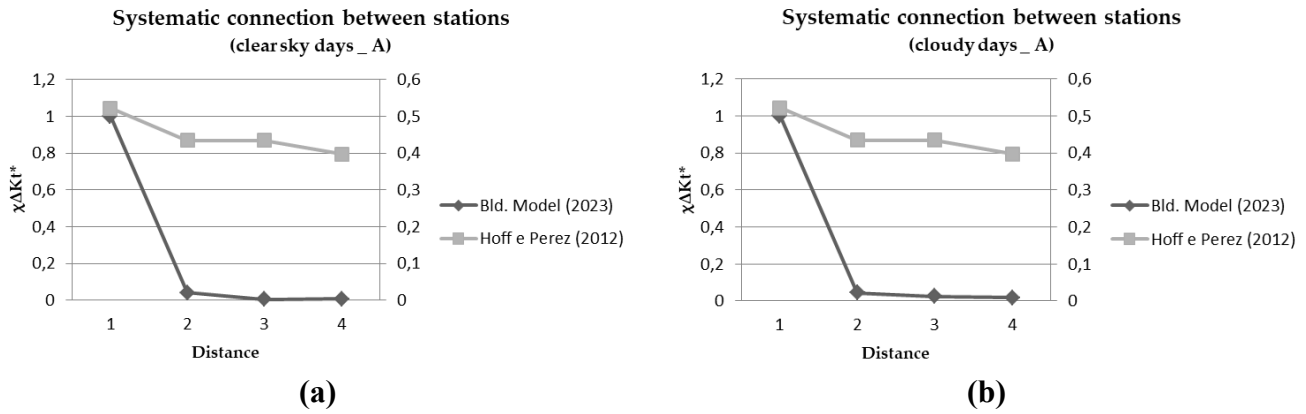


Figura A4: Distribuição de K_t^* e ΔK_t^* em função da hora do dia, para um intervalo de tempo de um minuto e uma amplitude de um dia, ao longo do dia 14 de setembro de 2012.



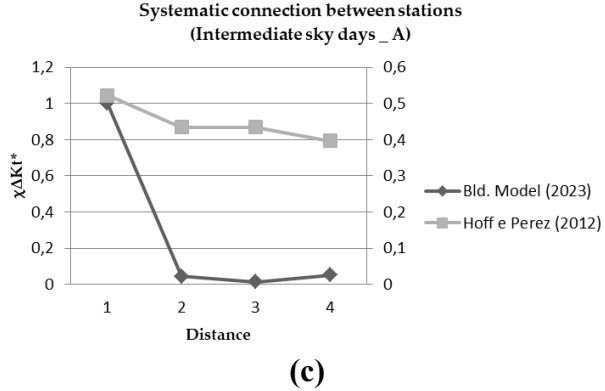


Figura A5: Coeficientes de correlação espacial de dois pontos na região centro-oeste de Moçambique para dias inaceitáveis do tipo: (a) céu limpo, (b) céu nublado e (c) céu intermédio.

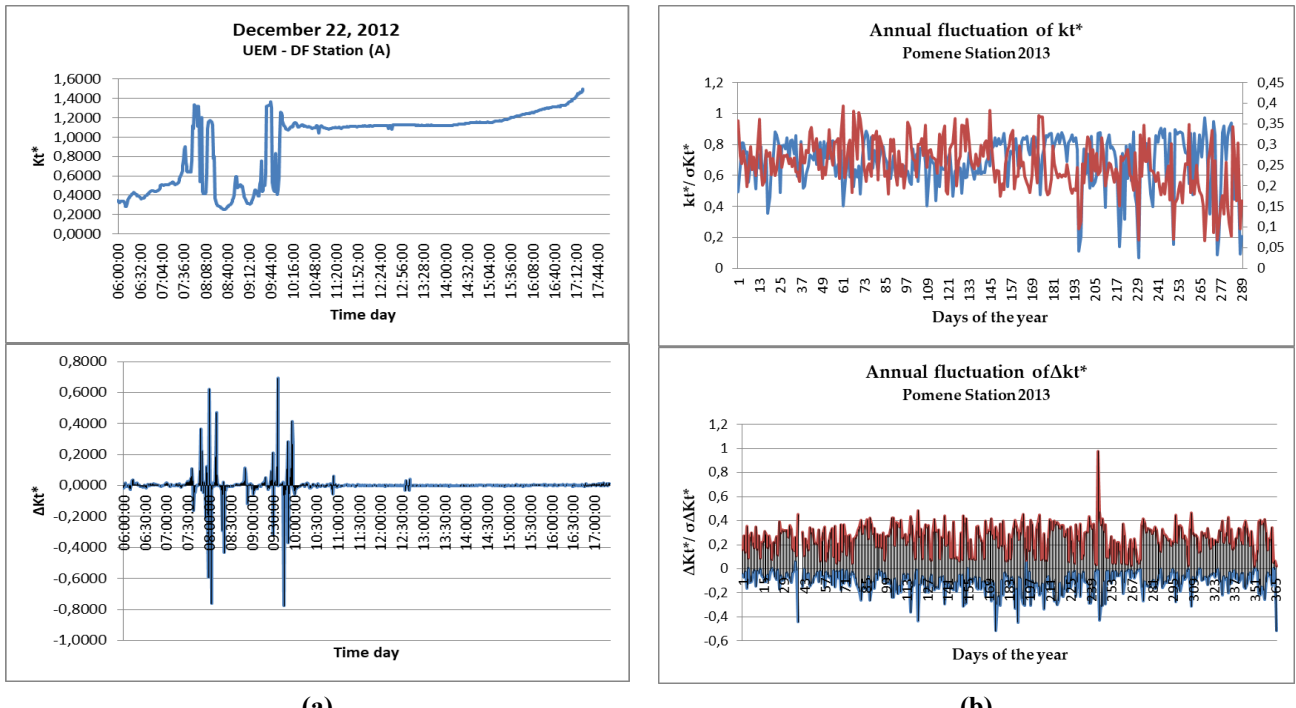
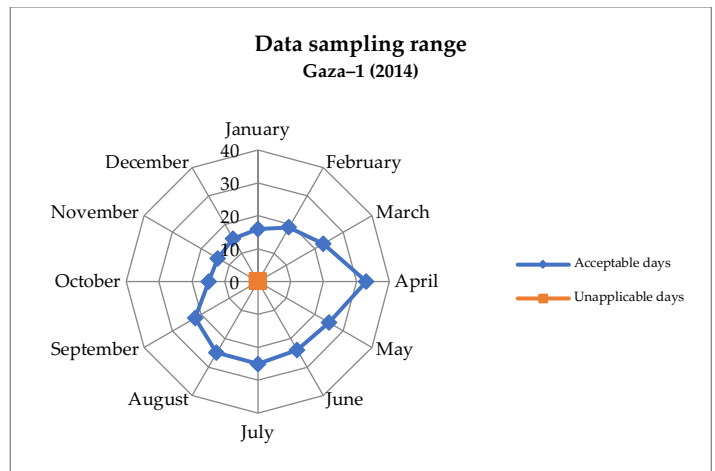
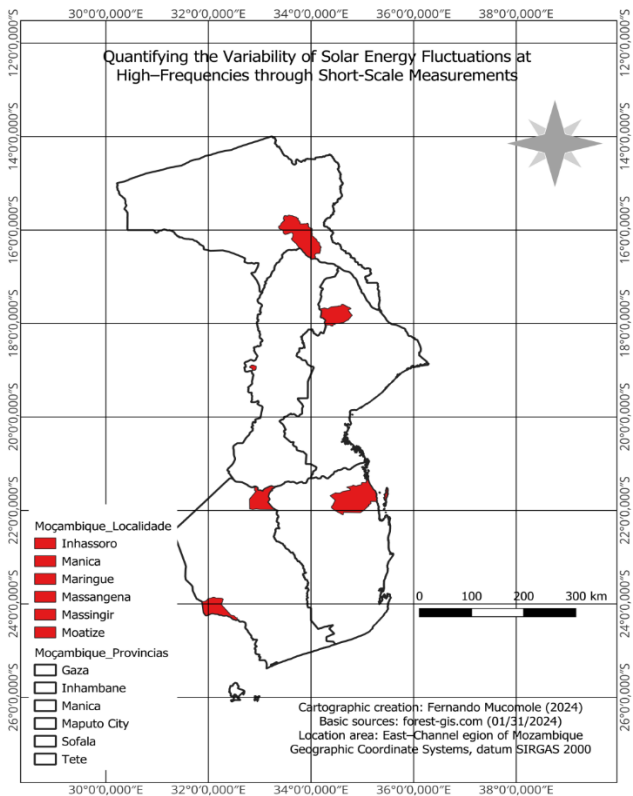


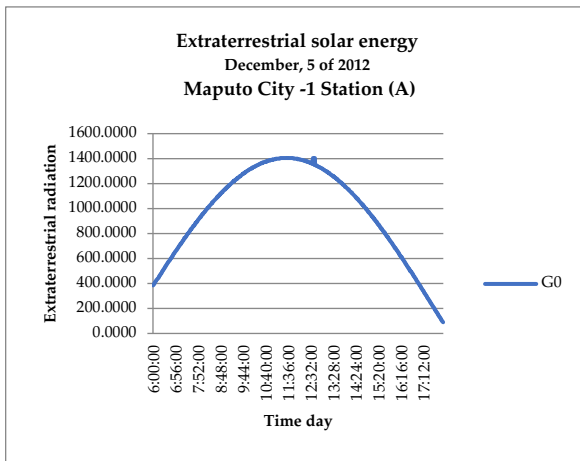
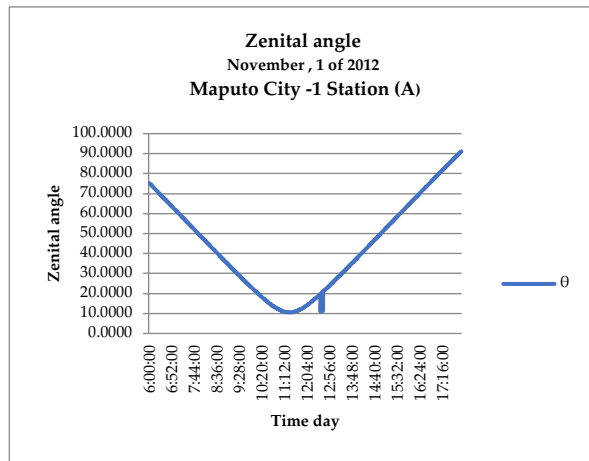
Figura A6: Distribuição de (a) K_t^* e ΔK_t^* em função da hora do dia, para: (a) Um intervalo de tempo de um minuto e uma amplitude de um dia (22 de dezembro de 2012); (b) um intervalo de tempo de um minuto e uma amplitude de um ano.



(a)

Figura A7: (a) Diagrama de acessibilidade à energia solar em termos de tipos de dias e Diagrama da estrutura de investigação de desenho estatístico, (b) Intervalo de dados de radiação solar global amostrados durante a campanha (exemplo da estação Gaza-1 em 2014) e (b) Escolha de datas na estação Barue-1 para o ano de 2014.

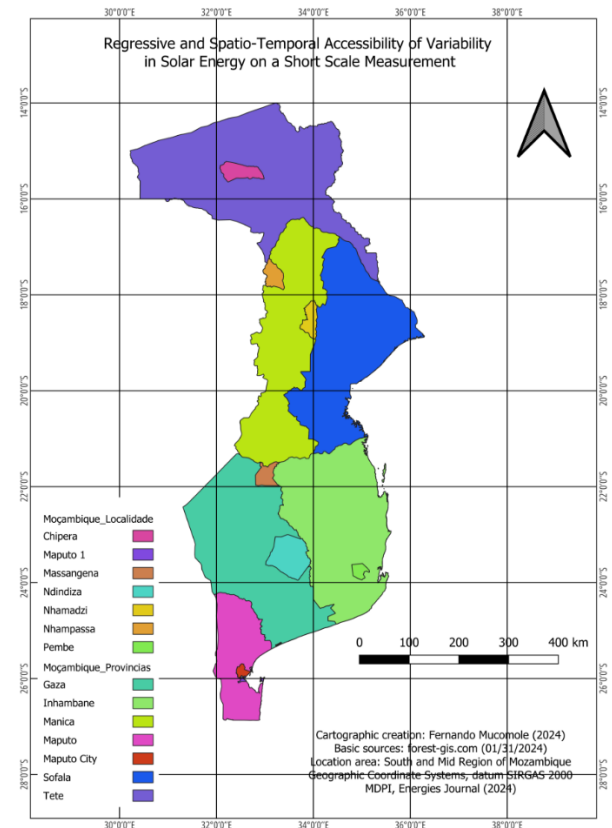
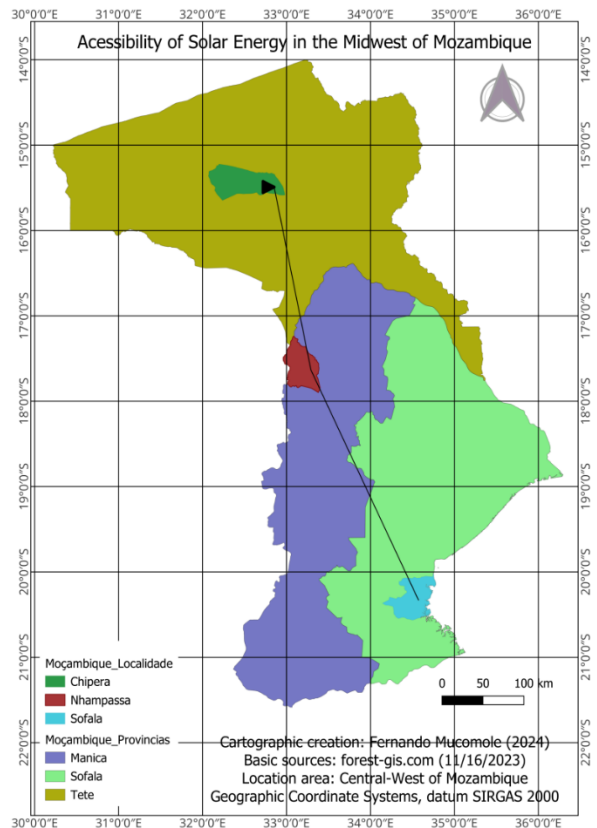
(b)



(a)

Figura A8: (a) Ângulo zenital (estação de Maputo–cidade: Ano 2012), (b) Exame dos padrões de radiação extraterrestre (estação de Maputo–cidade: Ano 2012).

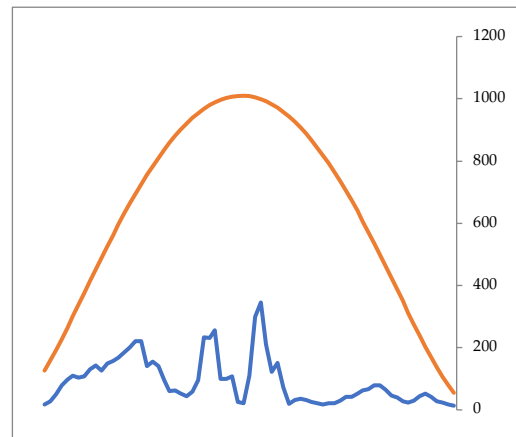
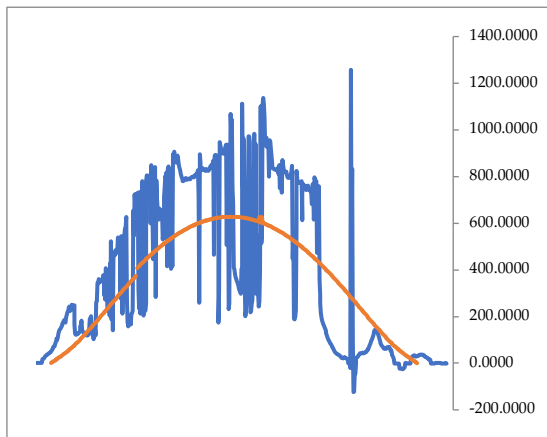
(b)

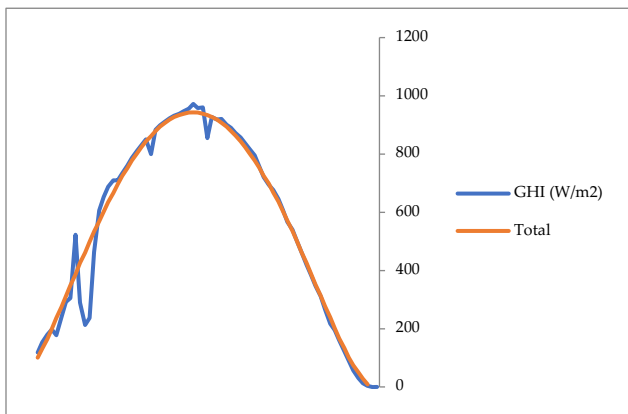


(a)

(b)

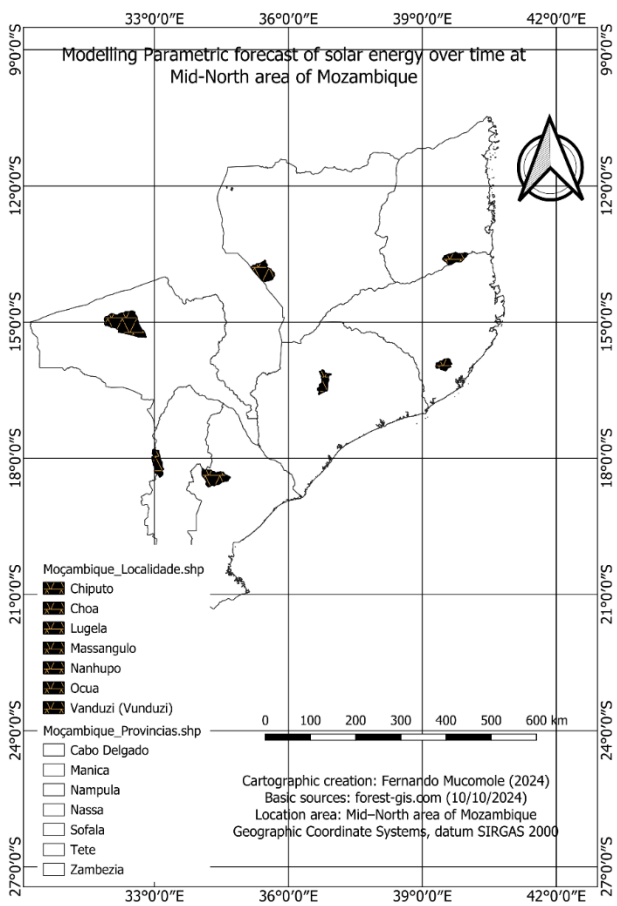
Figura A9: (a) Secção da área de estudo: Região Centro-Oeste de Moçambique Tamanho da amostra e (b) Secção da área de estudo: dimensão das regiões sul e centro da amostra de Moçambique.



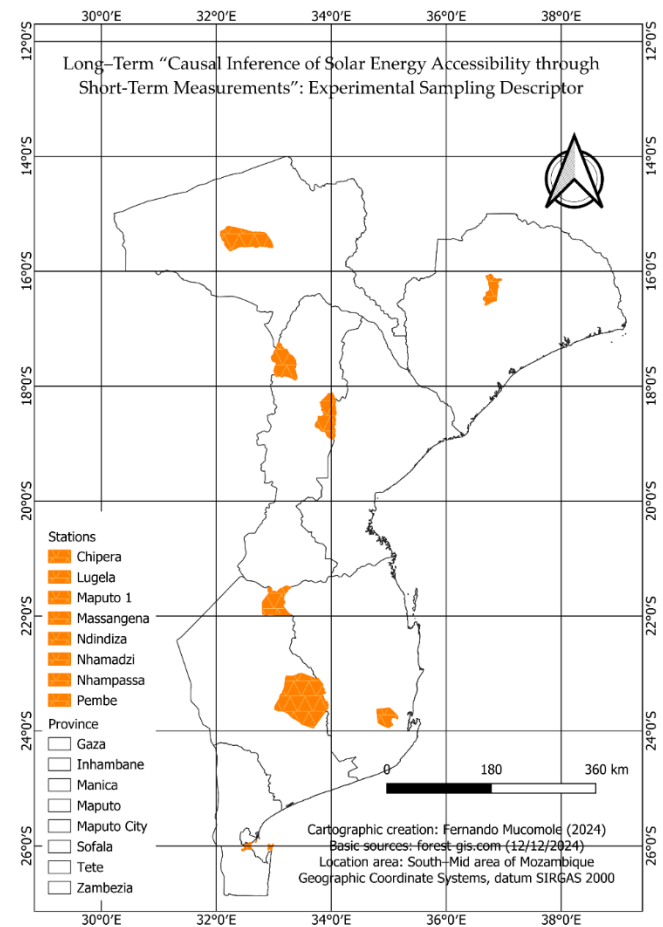


(c)

Figura A10: O contraste entre a radiação experimental e a radiação teórica está a ser examinado.



(a)



(b)

Figura A11: (a) Secção da área de estudo: região Centro-Norte de Moçambique Tamanho da amostra e (b) Área de estudo e recolha de dados.

Tabela A1: Localização dos postos de estudo.

| ID | Estação | Província | Torre | Longitude (X) | Latitude (Y) |
|------|---------------|-----------|-------|----------------|----------------|
| MZ11 | MZ11_Nhangau | Sofala | FUNAE | 35°2'18,72" E | 19°43'46,64" S |
| MZ21 | MZ21_Nhapassa | Manica | MceL | 33°13'0,79" E | 17°47'32,54" S |
| MZ06 | MZ06_Maravia | Tete | FUNAE | 31°40',3,3,7"E | 14°58'28,07" S |

onde MceL – significa Moçambique celular

Tabela A2: Quantificação da classificação dos tipos de dias

| Classificação | | | | |
|---------------|-----------|-----------|------------------------|------------------------|
| Mês | Claro | Nublado | Intermediário inferior | Intermediário superior |
| Abril | 2 | 6 | 2 | 0 |
| Maio | 0 | 5 | 3 | 2 |
| Junho | 2 | 3 | 3 | 2 |
| Julho | 5 | 1 | 1 | 3 |
| Agosto | 3 | 0 | 3 | 4 |
| Setembro | 2 | 2 | 2 | 4 |
| Outubro | 1 | 3 | 2 | 4 |
| Novembro | 7 | 0 | 1 | 2 |
| Dezembro | 0 | 4 | 5 | 1 |
| TOTAL | 22 | 24 | 22 | 22 |

ANEXOS

Table A3: Assessment of spatio-temporal variability on a short measurement scale.

| Type | Source | Data source | Interval | Contributions | Methods/ Models | Year | Location |
|----------------|--------------------------------------|-------------|---------------------|--|----------------------|------|-------------|
| <i>In situ</i> | (Mucomore <i>et al.</i> , 2023) | GHI | 1–10 min. | Temporal variability in the South | Analytical | 2023 | Mozambique |
| | (R. Perez <i>et al.</i> , 2016) | GHI | 0,01s | Spatial and Temporal Variability of GHI | Correlative | 2016 | USA |
| | (Stetz <i>et al.</i> , 2015) | GHI | 1 Hour | The Impact of Solar on Germany's Energy | Analytical | 2015 | Germany |
| | (Suri <i>et al.</i> , 2007) | GHI | 1 Hour | Solar electricity GHI prediction fluctuation | Analytical | 2007 | France |
| | (Hoff & Perez, 2010) | GHI | 1, 2, 3, 4 Hours | Modeling PV fleet output variability | PV fleet | 2010 | USA |
| | (Elsinga, B. and van Sark, W., 2014) | GHI | 1 min. | Urban rooftop PV systems & fluctuation | Correlative | 2014 | Netherlands |
| | (Calif <i>et al.</i> , 2013) | GHI | 0,01 s | Intermittency of GHI in a tropical climate | Correlative | 2013 | France |
| | (Lave <i>et al.</i> , 2013) | GHI | 20 s | Calibration of K_t^* as a function of distance | Correlative | 2013 | USA |
| | (Nwokolo <i>et al.</i> , 2022) | GHI | 1 Hour | Methods/formulas of K_t for regions | Gumbel probabilistic | 2022 | Africa |
| | (Nwokolo <i>et al.</i> , 2023) | GHI | 1 Hour | Impact of Climate Change on Solar PV | Physical models | 2023 | Africa |
| | (Almorox <i>et al.</i> , 2021) | GHI | 1 Hour | Extraterrestrial/clear-sky radiation | Analytical | 2021 | Spain |
| | (Klima & Apt, 2015) | GHI | 0,01 s | Geographic solar PV smoothing | Correlative | 2015 | USA |
| | (Lohmann <i>et al.</i> , 2016) | GHI | 15 min., 1 s, 0,01s | Day type behavior | Correlative | 2016 | Germany |
| | (Lohmann & Monahan, 2018) | GHI | 15 min., 1 s, 0,01s | Quantifying GHI in the short term | Correlative | 2018 | Germany |

| | | | | | | | |
|--|---|-----|---------------------|--|-----------------------|------|-------------|
| | (Lohmann & Monahan, 2017) | GHI | 15 min., 1 s, 0,01s | Quantification of the intermediate-sky | Correlative | 2017 | Germany |
| | (Fernando, D. M. Z, 2018) | GHI | 1–24 Hours | Mozambique K_t behavior | Analytical | 2018 | Brazil |
| | (de Souza <i>et al.</i> , 2019) | GHI | 1 Hour | GHI Vale do Rio Doce estimate | Analytical | 2019 | Brasil |
| | (Lonij V. P. <i>et al.</i> , 2013) | GHI | 1–24 Hours | Forecasts of solar power production | Correlative | 2013 | Canada |
| | (Luoma, J. <i>et al.</i> , 2012) | GHI | 0,01 s | K_t evaluation and correlation | Correlative | 2012 | Canada |
| | (Madhavan, B. L. <i>et al.</i> , 2016) | GHI | 0,01 s | Observe small-scale cloud inhomogeneity | Correlative | 2016 | Mexico |
| | (Marcos <i>et al.</i> , 2011) | GHI | 1 s | Power fluctuations: the PV plant/ filter | Correlative | 2022 | Spain |
| | (Mills, 2011) | GHI | 1 min. | Variability GHI Wide-Area Geographic | Correlative | 2011 | USA |
| | (Inman, R. H. <i>et al.</i> , 2013) | GHI | 0,01 s; 1 min. | Renewable energy integration | Forecasting | 2013 | UK |
| | (Hinkelman, L. M., 2011) | GHI | 1 min. | Characteristics of GHI Variability | Correlative | 2011 | USA |
| | (Van Haaren <i>et al.</i> , 2014) | GHI | 1 min. | Assessment of short-term PV variability | Empirical | 2012 | USA |
| | (Bailek <i>et al.</i> , 2020) | GHI | 1 min. | New model of GHI in Algeria | New prediction | 2020 | Algeria |
| | (Guermoui M. <i>et al.</i> , 2022) | GHI | 1 s, 1 min. | New temperature-based predicting GHI | Vector regression | 2022 | France |
| | (Rodriguez-Abreo, O., <i>et al.</i> , 2022) | GHI | 1 min. | Climate classification by neural irradiance | Irradiance models | 2022 | Mexico |
| | (Takilalte, A., <i>et al.</i> , 2020) | GHI | 5 min. | Estimate GHI data on tilted from horizontal | New approach | 2020 | Algeria |
| | (Toufik Arrif, <i>et al.</i> , 2022) | GHI | 1–24 Hours | Potential assessment of GHI | TVF-EMD | 2022 | Algeria |
| | (Obiwulu <i>et al.</i> , 2022) | GHI | 1 Hour | Modeling optimal tilt angle GHI of PV | Modeling correlate | 2022 | Africa |
| | (Hassan <i>et al.</i> , 2022) | GHI | 1 Hour | Forecasting of PV power production | Non-linear regressive | 2022 | Egypt |
| | (Y. Zhang <i>et al.</i> , 2018) | GHI | 1 min. | Validation of GFS day-ahead solar China | Correlative | 2018 | China |
| | (Arias-Castro <i>et al.</i> , 2014) | GHI | 1 min. | Anisotropic solar ramp rate correlations | Poisson | 2014 | USA |
| | (Aryaputera <i>et al.</i> , 2015) | GHI | 50 s | Very short-term irradiance forecasting | Kriking | 2015 | Singapore |
| | (Assuno, H. F., <i>et al.</i> , 2003) | GHI | 10 min. | Frequency of 5 min. GHI indexes by Beta. | Probabilities | 2003 | Brasil |
| | (C. Yang & Xie, 2012) | GHI | 1 min. | A ARX-based multi-scale PV forecast | ARX | 2012 | USA |
| | (D. Yang <i>et al.</i> , 2017) | GHI | 5 min. | Forecasting by covariance structures | Kriking | 2014 | Singapore |
| | (Wilcox <i>et al.</i> , 2010) | GHI | 1 Hour | Variability of the GHI in the united states. | SUNY model | 2010 | USA |
| | (Vijayakumar, 2004) | GHI | 1, 3 min., 1 Hour | Assessment of GHI in solar energy systems | HDKR model | 2004 | USA |
| | (Tovar <i>et al.</i> , 2001) | GHI | 1 min. | Dependence of one-minute GHI PDF | HELIOSAT and GISTEL | 2011 | Spain |
| | (Roversi, K., & Rampinelli, G. A., 2020) | GHI | 1–24 Hours | Grid connected inverter analysis | On grid | 2020 | Brazil |
| | (Sha & Aiello, 2020) | GHI | 1 min. | Decentralised, Energy Exchange Smart Grid | Monte Carlo method | 2018 | Netherlands |
| | (Keeratimahat <i>et al.</i> , 2017) | GHI | 5 min. | short-term variability, renewables penetrate | Analytical | 2017 | Australia |
| | (Koudouris <i>et al.</i> , 2018) | GHI | 1 Hour | GHI process for renewable manage | Stochastic | 2018 | Greece |
| | (Kreuwel <i>et al.</i> , 2020) | GHI | 15 min. | High frequency PV energy fluctuations | Analytical | 2020 | Netherlands |
| | (Habte <i>et al.</i> , 2020) | GHI | 1 Hour | Variability over America (1998–2017) | Correlative | 2020 | USA |
| | (Haegel <i>et al.</i> , 2017) | GHI | 1 Hour | Terawatt-scale photovoltaics | Correlative | 2017 | USA |

| | | | | | | |
|---|---------------------|---------------|---|-------------------|------|-------------|
| (Hoff & Perez, 2010) | GHI | 20 s | Quantifying PV power Output Variability. | Novel | 2010 | USA |
| (Ohtake <i>et al.</i> , 2013) | GHI | 1 Hour | Accuracy of the solar irradiance in Japan | Analytical | 2013 | Japan |
| (M. J. R. Perez & Fthenakis, 2015) | GHI | >1Hour | On the spatial decorrelation | Correlative | 2015 | USA |
| (Mills, 2011) | GHI | 1 min. | PV variability for Integrate Electric | Correlative | 2011 | USA |
| (Monjoly <i>et al.</i> , 2019) | GHI | 1 min. | Forecast Horizon and Solar Variability | MHFM | 2019 | France |
| (Nam, S., & Hur, J., 2019) | GHI | 1 min. | A hybrid spatio-temporal forecasting | Physical | 2019 | Korea |
| (Come Zebra <i>et al.</i> , 2021) | GHI | 1 Hour | Renewable Energy Tariff in Mozambique | Analytical | 2021 | Mozambique |
| (Dambreville, R. <i>et al.</i> , 2014) | GHI | 15 min. | Forecasting GHI by autoregressive model | Autoregressive | 2014 | France |
| (Dantas, 2018) | GHI | 1 Hour | Sizing a PV system | Physical | 2018 | Brazil |
| (Keeratimahat <i>et al.</i> , 2017) | GHI | 5 min. | Variability of utility-scale PV Australian | Correlative | 2017 | Australia |
| (Hummon <i>et al.</i> , 2012) | GHI | >1 Hour | Sub-Hour Solar Data for Power System | Static Spatial | 2012 | USA |
| (Ibanez <i>et al.</i> , 2002) | GHI | 1 Hour | Frequency Hourly and Daily K_t | Correlational | 2022 | Madison |
| (Lave <i>et al.</i> , 2012) | GHI | 0.01s, 1 min. | High-frequency GHI fluctuations geo | Correlational | 2012 | India |
| (Lefèvre <i>et al.</i> , 2013) | GHI | 1 min. | Estimating ground GHI in clear-sky | New model | 2013 | France |
| (Litjens <i>et al.</i> , 2018) | GHI | 1 min. | Assessment of residential PV power | Analytical | 2018 | Netherlands |
| (Barry <i>et al.</i> , 2017) | GHI | 5 s | Power fluctuations in solar-storage clusters | Correlative | 2017 | Germany |
| (Lan, H. <i>et al.</i> , 2018) | GHI | 1 Hour | Forecasting GHI along a navigation route | Correlative | 2018 | China |
| (R. Perez <i>et al.</i> , 2018) | GHI | 1 s | Solar Resource Variability | Different methods | 2018 | USA |
| (R. Perez, Rábago <i>et al.</i> , 2016) | GHI | 0,01 s; 1s | High PV penetration for effective electricity | Grig, correlate | 2016 | USA |
| (Zhou <i>et al.</i> , 2019) | GHI | 1 Hour | Assessment of the zero energy potential | Correlative | 2019 | USA |
| (Shakirov, 2019) | GHI and wind | 1 min. | Wind and solar power variability | Anisotropic model | 2019 | Russia |
| (Lucaciu <i>et al.</i> , 2016) | GHI and irradiative | 0,01s, 1 min. | Variability based on the clearness Index | Correlative | 2016 | Romania |
| (Y. Liu <i>et al.</i> , 2013) | GHI and wind | 1 Hour | China's solar and wind in a wide area | Correlational | 2013 | China |
| (Ciampi <i>et al.</i> , 2013) | GHI and Thermal | 1 min. | Energy efficiency in buildings: for thermal | Thermal | 2013 | Netherlands |
| (Jerez <i>et al.</i> , 2019) | GHI and wind | 1 Hour | Future temporal variability PV Europe | Analytical | 2019 | Spain |
| (Gueymard & Wilcox, 2011) | GHI and DNI | 1 Hour | Variability in direct irradiance (Sahara) | Correlative | 2010 | USA |
| (Qiu, R. <i>et al.</i> , 2022) | GHI hist. | 1 min. | Boosting model predicting daily GHI | Boosting | 2022 | China |
| (Lozano <i>et al.</i> , 2022) | GHI and DNI | 1 Hour | Analysis of cloud effects Mediterranean | Analytical | 2022 | Spain |
| (Belúcio, L. P. <i>et. al.</i> , 2022) | Insolation | 1 min. | GHI of Heatstroke | Estimative | 2014 | Brasil |
| (Hassan <i>et al.</i> , 2022) | PV systems | 1 min. | Energy affected by environmental factors | Physical models | 2022 | Egypt |
| (Yordanov, G. <i>et al.</i> , 2013) | Cloud speed | 15 min. | Temporal cloud-enhanced sunlight | Cloud enhanced | 2013 | Bulgaria |
| (Uti, M. N. <i>et al.</i> , 2023) | Ocean speed | 5 min. | Ocean renewable energy | K-means | 2023 | Malaysia |
| (Lave & Kleissl, 2013) | Cloud speed | 1 min. | Impact cloud speed solar variability | WVM | 2013 | USA |
| (Gallego, C. <i>et al.</i> , 2013) | Wind power | 0,1 s, 1 min. | large wind power ramp characterisation | WVM based | 2013 | USA |
| (Charabi & Gastli, 2012) | Solar energy | 1 Hour | Assessment of dust risk by proxy data. | MISR | 2012 | Oman |
| (Mazumdar <i>et al.</i> , 2014) | PV power | 0,01 s | Analysis of utility-scale solar PV power | Empirical model | 2014 | India |
| (Perpiñán & Lorenzo, 2011) | PV output | 1 min. | Variability of GHI, PV power time vs. wavelet | WVM | 2011 | Spain |

| | | | | | | | |
|-----------------------------------|---------------------------------|-------------------------|--|---|-----------------------|--------------|--------------|
| (Rapti, 2000) | Climate | 1 Hour | Atmospheric climatic turbidity, transparency | Atmospherical | 2010 | Greece | |
| (Salmanoğlu & ÇetiN, 2022) | Wind | 1–24 Hours | Harvest wind-Solar PV for Production | Wind | 2022 | Harvest | |
| (Anenberg <i>et al.</i> , 2017) | Air pollution | 1 Hour | Air pollution-related in Mozambique | Analytical | 2017 | Mozambique | |
| (Obiwulu <i>et al.</i> , 2020) | PV datta | 1 Hour | Modeling of back temperature by PV | Temperature model | 2020 | Africa | |
| (Neggers <i>et al.</i> , 2003) | Clouds speed | 1 min. | Size cumulus cloud populations | large-eddy SIM. | 2003 | USA | |
| (Xia <i>et al.</i> , 2023) | GHI | 1 Hour | Non-iterative decentralization in multi-micro grid systems | Non-iterative decentralized | 2023 | China | |
| (Di Fonzo & Girolimetto, 2023) | PV power | 1 Hour | Description of solar forecast rate reconciliation | NWP | 2023 | Italy | |
| (Jain <i>et al.</i> , 2023) | GHI, PV power | 1 Hour | System planning, variability and operational constraints | Different RES | 2023 | India | |
| (Z. Liu <i>et al.</i> , 2013) | PV power | 1 Hour | Spatial and temporal assessment of the PV potential of urban buildings | anisotropic sky diffuse | 2023 | China | |
| (Wu <i>et al.</i> , 2023) | PV power | 1 Hour | Analysis of energy consumption at various scales | Different methods | 2023 | China | |
| (Mol <i>et al.</i> , 2023) | GHI, images | 1 Hour | Observation of the variability of solar irradiation with cloud | Large eddy | 2023 | Netherlands | |
| (Zheng <i>et al.</i> , 2023) | PV, thermal, wind | 1 Hour | Power generation from multiple hybrid sources | Auto –Regression | 2023 | China | |
| (Shen <i>et al.</i> , 2023) | GHI, thermal | 1 Hour | Spatiotemporal analysis of surface energy change and heating | Long-wave | 2023 | China | |
| (Kong <i>et al.</i> , 2023) | GHI, thermal | 1 Hour | solar radiation for space heating | Convolutional network | 2023 | China | |
| (Sørensen <i>et al.</i> , 2023) | GHI | 1 Hour | Multivariate wind and solar power forecast | State-of-the art | 2023 | Denmark | |
| (Xu <i>et al.</i> , 2023) | GHI | 1 Hour | Environmental regulation | GTWR | 2023 | China | |
| (S. Zhang & Yan, 2022) | GHI | 1 Hour | State representation and identification for the structure of cavitation flow | CFD | 2023 | China | |
| (M. Yan <i>et al.</i> , 2020) | GHI | 1 Hour | Optimization of the energy distribution network between multimicrogrids | MISOCP | 2023 | China | |
| (Alharkan <i>et al.</i> , 2023) | Power energy | 1 Hour | Solar energy using architecture | CNN, LSTM, DSCLANet | 2023 | Saudi Arabia | |
| (W.-H. Chen <i>et al.</i> , 2022) | GHI and PV | 20 s, 1min. | PV power by NARX, Density Peak e cluster | Novel | 2022 | China | |
| Satellite | (Vindel <i>et al.</i> , 2020) | GHI | 1 Hour | Variability analysis of the GHI intertropical | REST2 model | 2019 | Spain |
| | (Tapia <i>et al.</i> , 2022) | GHI | 1 Hour | Variability of GHI in Ecuador | SFDA | 2022 | Ecuador |
| | (Zhu <i>et al.</i> , 2019) | Cloud | 1 Hour | Estimating sunshine duration cloud amount | New Physical model | 2020 | China |
| | (Q., & Xu, J., 2019) | Cloud | 1 Hour | Estimating Sunshine from a Geostationary | Correlative | 2019 | China |
| | (R. Perez <i>et al.</i> , 2012) | GHI | 20s, 15 min. | Short-term irradiance variability estimation | Correlative | 2012 | USA |
| | (Lorenzo, 2017) | GHI | 1 min., 1 Hour | Forecasting network, satellite imagery | Interpolation | 2017 | USA |
| | (Hoff & Perez, 2010) | Insolation | 0,01s; 1 s | Changes K_t two locations/ distance | Correlative | 2010 | USA |
| | (Hoff & Perez, 2011) | Insolation | 1 Hour | PV Power Output Variability | Correlative | 2011 | USA |
| | (Yu <i>et al.</i> , 2021) | Aerosol, water & vapors | 1 Hour | Effects of aerosols and water vapors in China | SSR | 2020 | China |
| | (Miller <i>et al.</i> , 2018) | GHI | 0,01 s; 1 min. | Short-term solar irradiance forecasting | Coupling | 2021 | Germany |
| | (Verbois <i>et al.</i> , 2023) | GHI | 1 min. | Improvement of satellite-derived GHI | Extrapolation/statist | 2023 | France |
| | (Amillo <i>et al.</i> , 2018) | GHI | 1 Hour | Satellite high GHI in South Africa | Correlative | 2018 | South Africa |
| | (Ayet & Tandeo, 2018) | GHI | 6 Hours | Now casting solar irradiance | NWP | 2018 | France |

| | | | | | | | |
|--|-------------------------------------|------------------------|--------|--|-----------------------|------|---------|
| | (Kumar, 2021) | GHI | 1 Hour | Variability using Meteosat satellite | Derived datasets | 2021 | India |
| | (Kühnert <i>et al.</i> , 2013) | GHI | 1 Hour | German Satellite PV Forecasting | Analytical | 2013 | Germany |
| | (Yu <i>et al.</i> , 2021) | Aerosol,water & vapors | 1 Hour | Effects of aerosols and water vapor in China | SSR | 2020 | China |
| | (Alharkan <i>et al.</i> , 2023) | GHI | 1 min. | Improvement of satellite-derived GHI | Extrapolation/statist | 2023 | France |
| | (Gutiérrez, C <i>et al.</i> , 2017) | GHI | 1 Hour | A multi-step PV production variability | Multi-Correlational | 2017 | Spain |

where: WVM – Wavelet variability model; NWM – Numerical weather model; NWP – Numerical Weather Prediction; HDKR – Hay, Davies, Klucher and Reindl model; MHFM – Multiscale hybrid forecast model; USA – United States of America; UK – United Kingdom; RES – Renewable Energy Sources; GTWR – Geographically and Temporally Weighted Regression; CFD – Computational Fluid Dynamics; MISOCP – mixed-integer second-order cone programming; CNN – convolutional neural network; LSTM – long short-term memory and DSCLANet – network followed by a self-attention mechanism network.

2.3. Especificações de cada ficheiro

De exemplo Os ficheiros “csv” intitulados “Chiputo_MZ06_PF”, “Vanduzi_1_MZ11_PF”, “Choa_MZ21_PF”, “Nanhupo_1_MZ24_PF”, “Nanhupo_2_MZ24_PF”, “Massagena_1_MZ25_PF” Z25_PF ”e“ Ocua_MZ03_PF ”s o referentes a amostras de dados estimados medidos e de par metros recolhidos em Chiputo na prov ncia de Tete, Vanduzi-1 na prov ncia de Sofala, Choa-1 e Choa-2 na prov ncia de Manica, Nanhupo-1 e Nanhupo-2 na prov ncia de Nampula, Massangena-1 e Massangena-2 na prov ncia de Niassa e Ocua na prov ncia de Cabo-Delgado.

Em cada ficheiro, a coluna A sob a escritura “Ano” refere-se ao ano dos exames m dicos no estado, a coluna B sob a escritura “m s” refere-se ao mesmo registo dos exames m dicos, a coluna C sob a escritura “Data” refere-se ao dia do registo m dico, a coluna D sob a escritura “data” refere-se ao dia acumulativo do registo m dico, a coluna e sob a escritura “GHI” refere-se   sondagem global no di rio de comunica o social relacionado com o m dico registado em intervalos de 1 a 10 minutos, a coluna F escritura “ID” refere-se   identifica o atribu da pelo investigador ao posto de medicamentos, a coluna G sob a escritura “Est o o” refere-se ao nome do posto de medicamentos, a coluna H sob a escritura “Prov ncia” refere-se   prov ncia de localiza o do posto de medi es, a coluna I sob a escritura “Torre” refere-se ao nome da torre em que ocorreu a queda do medicamento (propriet rio da torre), a coluna J sob a escritura “C digo” refere-se ao c digo do propriet rio da torre no pa s, a coluna K sob a escritura “Longo -se   longitude do local de medi o, a coluna L sob a escritura “Lat. (Y) refers to the latitude of the medical site, the column M under scripture “altitude” refers to altitude to the level of the sea of the measurement location, the column N under scripture “ WV_AOT(675_nm) ”refers the exact wavelength of optical aerosol thickness (675 nm) in nanometers, the column O under deed “W V_AOT (440_NM)” refers to the exact

wave comparison of aerosol optical thickness (440 nm) in nanometers, column P under deed “AOT(675_nm)” refers to the optical spot of solar energy in the 675 nm wave composts, the Q column “AOT(440_nm)” refers to solar energy optics feature in the 440 nm wave compliances, column R under deed “PW(cm)” refers to the measured precipitating water, the S column S “Pre(mbars)” refers to Mili Bars, colu96mn T under Scripture “O3(cm)” refers to the thickness of the ozone layer concentration, the column U under deed “N(cm)” refers to NO2 and other ed gases, finally the column V under deed “temperature_(K)” refers to local temperature.

Table A4. Solar radiation and atmospheric parameters.

| Station | GHI (W/m ²) | Longitude (0) | Latitud e (0) | AOT (675 nm) | AOT (440 nm) | Agua precipitáv el (cm) | Pressão (mbars) | Ozone (cm) | NO ₂ (cm) | Temperatu ra (K) |
|--------------|-------------------------|---------------|---------------|--------------|--------------|-------------------------|-----------------|------------|----------------------|------------------|
| Ocua | 351.13 | 39.39 | -11.55 | 0.15 | 0.29 | 2.69 | 958.61 | 2.62 | 0.0014 | 272.99 |
| Chiputo | 399.67 | 31.67 | -14.97 | 0.14 | 0.30 | 2.13 | 1016.35 | 2.63 | 0.0014 | 299.89 |
| Vanduzi | 477.19 | 35.04 | -19.73 | 0.18 | 0.34 | 3.47 | 1010.30 | 2.83 | 0.0018 | 308.26 |
| Choa-1 | 355.49 | 33.24 | -17.79 | 0.14 | 0.30 | 2.13 | 1016.08 | 2.63 | 0.0014 | 299.96 |
| Choa-2 | 354.66 | 33.24 | -17.79 | 0.14 | 0.30 | 2.13 | 1016.08 | 2.63 | 0.0014 | 299.96 |
| Nanhupo-1 | 352.64 | 39.51 | -15.97 | 0.15 | 0.29 | 2.59 | 958.43 | 2.61 | 0.0015 | 272.99 |
| Nanhupo-2 | 349.65 | 39.51 | -15.97 | 0.15 | 0.29 | 2.59 | 958.44 | 2.61 | 0.0015 | 272.99 |
| Massangulo-1 | 345.91 | 35.44 | -13.91 | 0.15 | 0.30 | 2.59 | 958.42 | 2.61 | 0.0015 | 272.99 |
| Massangulo-2 | 430.09 | 35.44 | -13.91 | 0.15 | 0.30 | 2.59 | 958.42 | 2.61 | 0.0015 | 272.99 |
| Lugela | 367.99 | 36.71 | -16.47 | 0.14 | 0.29 | 2.60 | 958.35 | 2.61 | 0.0014 | 272.99 |